

Simultaneous measurement of spatially separated forces using a dual-cantilever resonance-based touch sensor

Jack V. Phan, Robert Hocken, Stuart T. Smith, and Russell G. Keanini^{a)}

Precision Engineering Laboratory, Department of Mechanical Engineering and Engineering Science, University of North Carolina at Charlotte, Charlotte, North Carolina 28223

(Received 31 May 2001; accepted for publication 5 November 2001)

A simple device for simultaneously measuring two spatially separated contact forces is described. The device uses a monolithic dual-cantilever touch sensor driven by a piezoelectric PZT actuator. A phase-locking method allows measurement of resonant frequency shifts at constant phase, based on the strain response of a second attached PZT. Calibration and force measurement procedures are developed to extract applied contact forces from the dual-cantilever's coupled, nonlinear response. Based on a preliminary calibration, the present device exhibits maximum relative measurement error on the order of 6%. Procedures for reducing this error are described. © 2002 American Institute of Physics. [DOI: 10.1063/1.1431439]

I. INTRODUCTION

Resonance-based sensors are used in a variety of applications including material property measurement, mechanical characterization of fluids and solids, flow and liquid level metering and control, surface metrology, and friction force measurement.¹⁻³ A number of these applications rely on simultaneous detection of two force components at a point or on simultaneous measurement of two forces (or force-related quantities) at spatially distinct points. Examples of the former include mesoscale³ and micro- and nanoscale⁴ investigations of friction and wear while examples of the latter include fluid flow anemometry, flow metering and control, and high-sensitivity accelerometry.¹

With regard to anemometry, previous methods have used separate sensors attached to vibrating pipe sections or internal vibrating vanes to extract total volumetric flow rates.¹ Recent work,^{5,6} however, has focused on developing a resonance-based method for measuring *local* fluid velocities. Here, based on the measurement principle⁵ underlying Pitot tube anemometers, simultaneous measurement of flow-induced forces at two near-coincident points is required. The present study continues work in this direction by developing methods for measuring simultaneously applied forces on a dual-cantilever resonance sensor.

Vibrational coupling and nonlinear response can compromise the accuracy of simultaneous resonance-based force measurements,^{3,7,8} particularly when a single cantilever is used. Although these limitations are now recognized, relatively little work has been reported on methods for accommodating and minimizing these effects. For example, the device recently reported by Chui *et al.*⁴ appears to represent the only resonance-based method presently available for decoupling lateral and vertical force measurements at a point. (A nonresonant method for decoupling simultaneous force measurements at a point was recently reported by Hendriks and Vellinga.^{3,7}) Of particular importance in treating nonlinearity

and coupling effects is development of appropriate calibration and inversion procedures, where calibration refers to measurement of a beam's frequency response to known imposed loads and where inversion refers to determination of an unknown force, given a measured response and a known calibration.

This article describes development of a relatively simple resonance-based method for simultaneously measuring forces at two points. As shown in Fig. 1, the device incorporates a monolithic dual-cantilever driven by a PZT actuator. Decoupling of the dual-cantilever's nonlinear response is achieved in part by ensuring that each cantilever has a distinct resonant frequency (achieved here using differing beam lengths), and in part by electronic filtering. Calibration and data inversion procedures are described in detail and measurement error is assessed. In addition, methods for improving measurement accuracy are briefly described.

II. DESIGN AND CONSTRUCTION OF DUAL-CANTILEVER PROBE

The device is designed to simultaneously measure two forces, F_1 and F_2 , where F_1 is applied longitudinally to the long beam and F_2 is applied laterally to the short beam. Refer to Fig. 1. This configuration is designed for future application in an enclosed Pitot tube,^{5,6} where the short beam will detect local static pressure while the long beam detects local stagnation pressure. Other configurations are possible including triple-beam, yaw-correcting measurement of three pressures, or single beam measurement of static or stagnation pressure.

Measurement of the forces acting on each of the cantilever beams requires: (i) that the beams' resonant frequencies are decoupled; (ii) that measured resonant frequency shifts can be related to known loads, i.e., a calibration developed; and (iii) that the calibration allows data inversion, i.e., measured frequency shifts can be used to determine the unknown forces. We will consider the first requirement as well as

^{a)}Corresponding author; electronic mail: rkeanini@uncc.edu

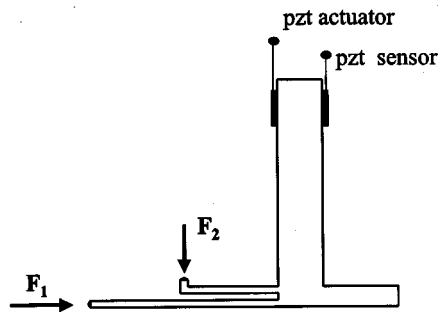


FIG. 1. Schematic of the dual-cantilever touch sensor.

probe construction in this section and will describe calibration and data inversion in Sec. IV.

A. Probe construction

In order to ensure relatively low thermal expansion and resistance to melting both during fabrication and in high-temperature applications,^{5,6} the device is machined from Carbide GC-015 (15% cobalt, 85% tungsten carbide by weight). For ease of fabrication and testing, the probe's dimensions are relatively large. However, the calibration and inversion method, and the results described below are expected to apply to smaller devices. Actuator and pick-up piezoelectric sensors are bonded to opposite sides of the dual-cantilever's vertical arm using M-BOND 200 adhesive. The sensors are fabricated using rectangular (3 mm wide, 10 mm long and 1 mm thick) lead-zirconate-titanate (PZT) plates that are oriented longitudinally along the cantilever's vertical arm. While both transverse and longitudinal modes are excited within the dual cantilever, the PZTs' size, orientation, and placement have not been optimized to excite or detect either of these modes. As noted in Sec. II C below, measurements are based on detected transverse modes.

B. Approximate design equations and decoupled beam response

As shown by Vidic *et al.*,² transverse or longitudinal excitation can be used to drive the dual cantilever. Although the analysis in Vidic *et al.*² is not strictly applicable to the beams in the present device, for preliminary design purposes, it provides useful qualitative information on the behavior of resonance frequency as a function of beam geometry and beam material properties. Thus, the longitudinal resonant frequency for either beam is estimated as⁸

$$\omega_j = \frac{(2j-1)\pi}{2L} \left(\frac{E}{\rho} \right)^{1/2}, \quad (1)$$

where ω_j is the frequency of j th longitudinal mode, L is the beam length, and E and ρ are the beam's elastic modulus and density. Likewise, transverse natural frequencies can be estimated using⁹

$$\omega_{lj} = \frac{A g_j}{2\pi}, \quad (2)$$

where g_j is the natural frequency factor for the j th mode, $A = (EI/\rho L^4)^{2/3}$ is the beam's cross-sectional area, and I is

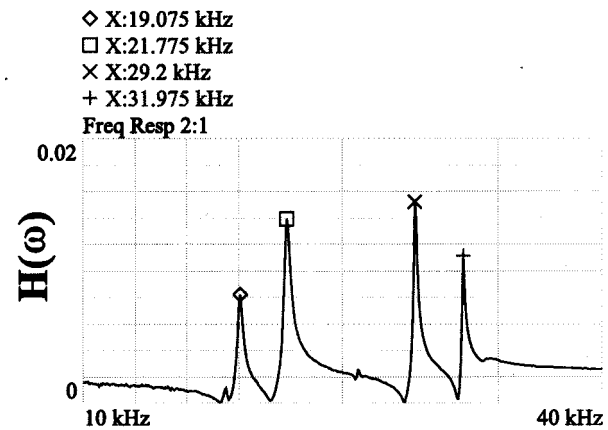


FIG. 2. Typical system frequency response function.

the beam's second moment of inertia. If necessary, shifts in the first longitudinal resonant mode due to contact-induced added mass and stiffness effects can also be estimated.²

The response characteristic of each cantilever beam over a small frequency band about a resonance depends on the beam and boundary conditions' compliance, inertia, and damping. Since these parameters in turn generally vary with the contact force applied to the beam's tip, the sensor's resonance frequencies and associated response characteristics also vary. However, since contact force-induced variations in compliance, inertia, and damping are fixed and repeatable for a given sensor, variations in resonance and response can be directly and unambiguously related (via calibration) to the contact force. As an illustration, consider sealed Pitot tubes^{5,6} in which each beam tip contacts an elastic, pressure-sensitive diaphragm. Increasing fluid pressure on the diaphragm reduces the compliance of the elastic (Hertzian) contact between the tip and diaphragm while likely increasing structural/interface damping and inertial loading (due to increased area of contact). Barring contamination and material or structural changes, however, compliance, inertia, and damping variations remain fixed and variations in sensor response depend only on pressure. Note that theoretical treatments relating applied force on a dual cantilever to transverse or longitudinal resonance frequencies apparently have not been reported.

From Eqs. (1) and (2), it is apparent that in the present design where both beams have identical cross sections, well-separated resonant frequencies require significant differences in beam length L . As shown in Fig. 1, a long-beam length twice that of the shorter was chosen. In applications requiring equal or near-equal beam lengths, vibrational decoupling can be ensured by mismatching beam materials (E/ρ), and/or beam cross sections.

C. Phase locking

The dual-cantilever's frequency response function $H(j\omega)$ is first determined under nonloaded conditions, $F_1 = F_2 = 0$, over a range of excitation frequencies. As shown in Fig. 2, for the resonator described here, the amplitude ratio $|H(j\omega)|$ exhibits four peaks, corresponding to the first four

system resonances. The two lowest frequency peaks remain fixed at all forcing frequencies and correspond to modes excited in a heavy clamp used to fix the dual-cantilever probe. The highest and next highest peak frequencies, $\omega_2^{(o)}$ and $\omega_1^{(o)}$, by contrast, correspond, respectively, to the short and long beam's lowest order transverse resonant frequencies and are sensitive to loading. In particular, under load, effective added stiffness increases each beam's resonant frequency, which, in turn, produces shifts, $\Delta\omega_1$ and $\Delta\omega_2$, in $\omega_1^{(o)}$ and $\omega_2^{(o)}$.

A standard phase locking circuit is used to detect the frequency shifts $\Delta\omega_1$ and $\Delta\omega_2$, as a function of the applied loads F_1 and F_2 . The principal of operation is as follows. First, the phases $\phi_1^{(o)}$ and $\phi_2^{(o)}$ and corresponding long and short beam resonant frequencies $\omega_1^{(o)}$ and $\omega_2^{(o)}$ are measured under nonloading conditions. A load combination, (F_1, F_2) , is then applied, and a corresponding frequency response function generated by exciting the PZT actuator over narrow bands of frequency near $\omega_1^{(o)}$ and $\omega_2^{(o)}$. Due to changes in effective added stiffness, the resonance frequencies shift to $\omega_1(F_1, F_2)$ and $\omega_2(F_1, F_2)$; these in turn are determined from the updated frequency response function using the constant phases $\phi_1^{(o)}$ and $\phi_1^{(o)}$.

III. EXPERIMENTATION

A longitudinal force, F_1 , and transverse force, F_2 , are simultaneously applied to the tips of the long and short beams, respectively. Due to the short beam's relatively low sensitivity to transverse loading, this choice provides a fairly robust test of the dual-cantilever's capabilities. While any combination of purely transverse and longitudinal loading can be applied to the beam tips, oblique loading introduces two force components at each tip, necessitating a more involved calibration procedure. During calibration (see below), the range of applied forces is limited to 0.035 to 0.36 N.

The forces are applied through flexure-based load cells, each of which are monitored using a linear variable differential transformer (LVDT). Here, a micrometer presses a small spring (stiffness = 2.2×10^6 N/m) connected to the LVDT (sensitivity = $50 \text{ mV}/\mu\text{m}$) which in turn contacts the beam tip. Voltage from the inductive gage is measured via a volt meter (accuracy = 0.02 mV) while a digital signal analyzer (DSA; Hewlett-Packard model HP 35665 A) creates the driving signal and detects the response at the sensing PZT. It is important to note that contact forces must be applied by the same means during both calibration and measurement. For example, in the present set of experiments (and as alluded to in Sec. II B), since the sensor's response depends in part on the spring's spring constant, calibration, and force measurements use the same spring and associated attachments. The DSA also determines the phase lags $\phi_1^{(o)}$ and $\phi_2^{(o)}$ between the driving signal and the unloaded beams and then measures the frequencies ω_1 and ω_2 (at these phase lags) as functions of the applied forces F_1 and F_2 . A schematic of the experimental setup is shown in Fig. 3.

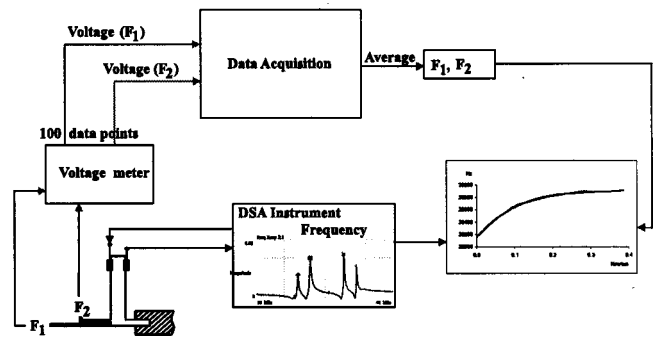


FIG. 3. Schematic diagram of force measurement system.

IV. CALIBRATION AND DATA INVERSION

A. Calibration

The calibration procedure constitutes a two-step process and results in the creation of two calibration surfaces, $\omega_1 = \Omega_1(F_1, F_2)$ and $\omega_2 = \Omega_2(F_1, F_2)$. In the first step, a set of frequency measurements is obtained by incrementally varying F_1 (the force on the long beam) from F_{\min} ($=0.036 \text{ N}$) to F_{\max} ($=0.35 \text{ N}$) while holding F_2 (the force on the short beam) fixed at, say, $F_2^{(i)}$. The resulting measurements of ω_1 and ω_2 are then fit to third order polynomials, giving the curves $\omega_1 = \omega_1(F_1, F_2^{(i)})$ and $\omega_2 = \omega_2(F_1, F_2^{(i)})$. This process is repeated at a series of fixed values $F_2^{(i)}$, where $F_{\min} \leq F_2^{(i)} \leq F_{\max}$. In the second step, two-dimensional linear interpolation is used to generate the surfaces $\Omega_1(F_1, F_2)$ and $\Omega_2(F_1, F_2)$; these are saved digitally at fixed intervals in F_1 and F_2 . As described by Phan,⁵ polynomial fitting and linear interpolation programs used for calibration were written and validated against commercial software. Contour plots of the surfaces Ω_1 and Ω_2 are shown in Figs. 4 and 5.

B. Data inversion

Determination of two unknown forces, F_1 and F_2 , given frequency measurements ω_1 and ω_2 , requires inversion of the calibration relationships $\omega_1 = \Omega_1(F_1, F_2)$ and $\omega_2 = \Omega_2(F_1, F_2)$. The inversion procedure, and several poten-

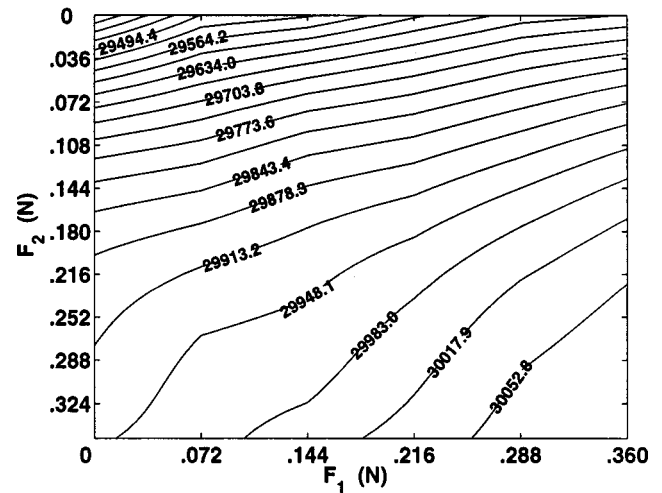


FIG. 4. Contour plot of calibration surface $\omega_1 = \Omega_1(F_1, F_2)$. Frequencies shown in Hz.

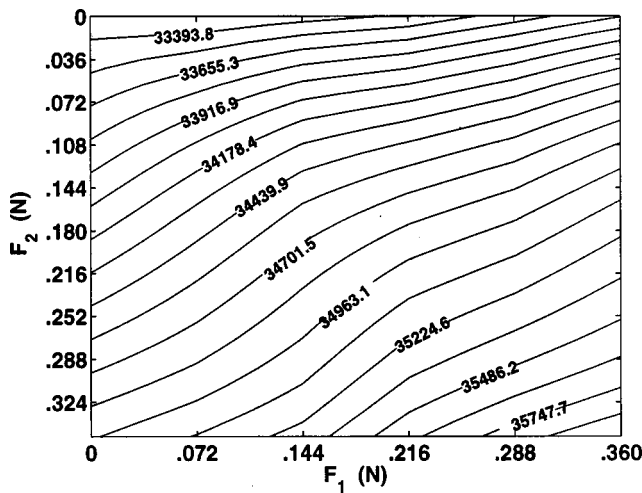


FIG. 5. Contour plot of calibration surface $\omega_2 = \Omega_2(F_1, F_2)$. Frequencies shown in Hz.

tial pitfalls, are perhaps most easily described in geometric terms. Thus, consider the surfaces Ω_1 and Ω_2 shown in contour in Figs. 4 and 5. Given a measured value of ω_1 , which we will denote as $\omega_1^{(m)}$, then the set of all possible forces (F_1, F_2) capable of producing $\omega_1^{(m)}$ defines a curve $\Gamma_1^{(m)}$, where $\Gamma_1^{(m)}$ is the intersection between the plane $\omega = \omega_1^{(m)}$ and the surface Ω_1 . Likewise, the set of all force pairs capable of producing the observed value of $\omega_2 = \omega_2^{(m)}$ defines a similar curve $\Gamma_2^{(m)}$ on the surface Ω_2 .

Given the curves $\Gamma_1^{(m)}$ and $\Gamma_2^{(m)}$, representing a set of two nonlinear equations in two unknowns, F_1 and F_2 , then three potential outcomes must be considered: (1) no solutions exist; (2) one solution exists; or (3) more than one solution exists. The first possibility can be dismissed by recognizing that the curves $\Gamma_1^{(m)}$ and $\Gamma_2^{(m)}$, projected on the plane $\omega = 0$, must cross at least once. Since all points on both curves are experimental realizations of the dual-cantilever's response to applied forces, any pair of observed frequencies must correspond to at least one pair of imposed forces, i.e., a point (F_1, F_2) common to both curves. (This assumes that the unknown forces lie within the range of forces used to generate the calibration.)

Considering the third possibility, that of multiple solutions, we find that in most cases, the curves $\Gamma_1^{(m)}$ and $\Gamma_2^{(m)}$ actually cross at two points, i.e., two distinct pairs of applied force are capable of producing a nominally identical pair of resonant frequencies. Prior to discussing this observation, it is useful to briefly differentiate between instances when the curves actually cross and when the curves touch or appear to touch tangentially. The first case, indicated when data points on each curve lie fore and aft of the crossing point, signals the existence of an actual root or solution. The second case could indicate a real solution, but more likely represents a spurious solution produced, e.g., by suboptimal resolution in frequency shift measurements and/or interpolation error introduced during calibration. Fortunately, extensive tests suggest that in this system, tangential incidence never occurs. Thus, considering the observation that most curves cross twice, it is clear that this feature reflects the system's nonlin-

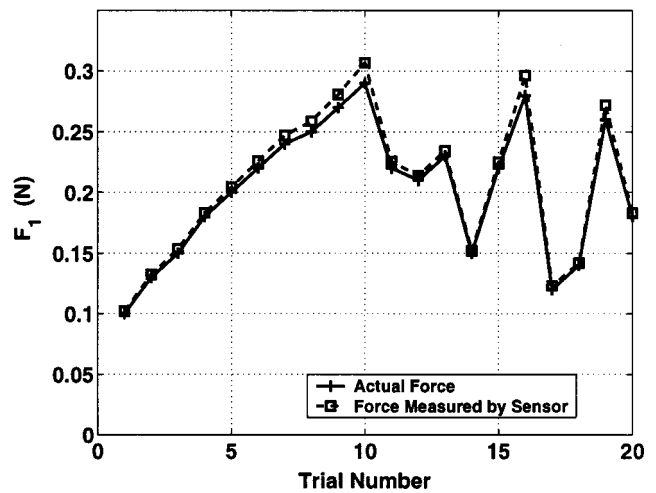


FIG. 6. Comparison of forces measured by dual-cantilever touch sensor with actual imposed forces. Twenty simultaneous force measurements were performed. The forces F_1 shown here are those on the long beam while those shown in Fig. 7 (F_2) are those on the short beam.

earity, and in particular, its nonunique response to imposed forces.

In order to determine which solution should be used, ancillary information regarding, e.g., the relative magnitudes of the forces F_1 and F_2 may in many cases be used to eliminate the inappropriate solution. For example, and as mentioned, the present device will eventually be incorporated in a Pitot-tube-based anemometer;^{5,6} in this case, since the sum of the static and dynamic pressures on the long beam are larger than the static pressure on the short beam, $F_1 > F_2$. As another example, the present device could be used for high precision fluid density measurements. In this case, the cantilevers would be aligned vertically, parallel to the gravity field, so that a slightly higher hydrostatic force on the long beam would again lead to the constraint $F_1 > F_2$. Alternatively, nonunique solutions can be circumvented at the calibration stage by using data that satisfy any given constraint between F_1 and F_2 . In cases where no such constraint exists, it may be necessary to validate the data inversion procedure over the entire range of observable frequencies; here, spurious solutions are identified and flagged prior to actual force measurements.

V. RESULTS AND DISCUSSION

In order to test the dual-cantilever method, 20 different, arbitrarily chosen pairs of known forces, $(F_1^{(a)}, F_2^{(a)})|_1, \dots, (F_1^{(a)}, F_2^{(a)})|_{20}$, are applied to the dual cantilever and the corresponding resonant frequencies measured. Each of the 20 pairs of measured resonant frequencies are then input into the data inversion program which determines 20 associated pairs of estimated force, $(F_1^{(e)}, F_2^{(e)})|_1, \dots, (F_1^{(e)}, F_2^{(e)})|_{20}$. Comparisons of the actual and estimated forces for each of the 20 trials are shown in Figs. 6 and 7. Defining maximum relative errors, E_1 and E_2 , as

$$E_1 = \max \left| \frac{F_{1i}^{(e)} - F_{1i}^{(a)}}{F_{1i}^{(a)}} \right|, \quad i = 1, \dots, 20$$

and

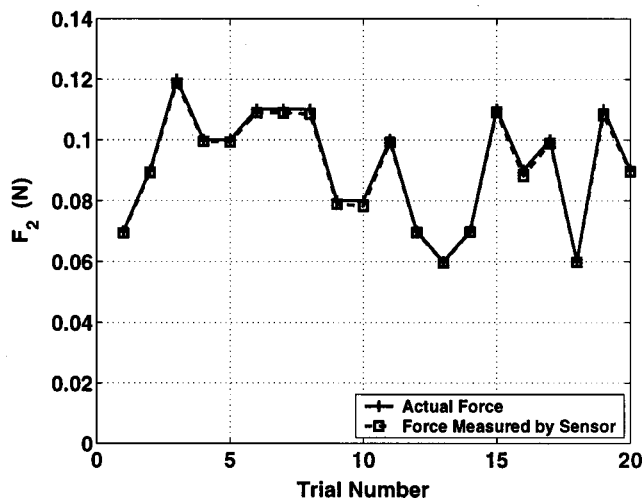


FIG. 7. Comparison of forces measured by dual-cantilever touch sensor with actual imposed forces. See the caption to Fig. 6 for an explanation.

$$E_2 = \max \left| \frac{F_{2i}^{(e)} - F_{2i}^{(a)}}{F_{2i}^{(a)}} \right|, \quad i = 1, \dots, 20$$

we see from Fig. 8 that E_1 is approximately 6% while E_2 is on the order of 2%.

The effect of interpolation error is apparent in Fig. 8, where the largest errors occur at (interpolated) points (F_1, F_2) that are somewhat removed from experimental points used in calibration. In order to improve the accuracy of dual-cantilever-based force measurements, the accuracy of the calibration between force and frequency can be improved. This in turn requires enhanced frequency shift measurement resolution and reduction of interpolation error. Frequency shift measurement resolution can be improved by using larger samples when determining average frequency shifts [at any given set of imposed forces, (F_1, F_2)], and by reducing measurement uncertainty due, e.g., to ambient temperature variations and stray vibration. [Note that the frequency shifts used in the present calibration each represent an average over 100 trials.] Interpolation error can be reduced by increasing the number of data points used in calibration and through use of higher order interpolation schemes.

Development of a resonance-based method for simultaneously measuring two spatially discrete forces provides the basis for developing a *local*, resonance-based flow anemom-

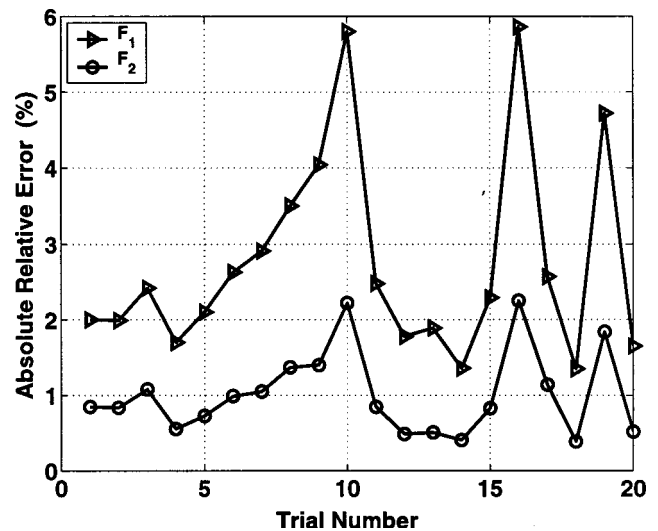


FIG. 8. Absolute relative measurement errors for simultaneous force measurements shown in Figs. 6 and 7.

etry. More generally, and as shown above, the nonlinear, coupled response of cantilever-based measurements can lead to nonunique extraction of forces. Although nonlinear coupling characterizes many cantilever-based measurements, e.g., friction force microscopes,⁷ the potentially ubiquitous nature of this problem has not been considered in the literature. In addition, development of robust calibration and inversion procedures is critical to tackling problems associated with nonlinear coupling.

ACKNOWLEDGMENT

Support for this work, provided by the National Science Foundation, Grant No. DMI 9712818, is gratefully acknowledged.

¹R. M. Langdon, *J. Phys. E* **18**, 103 (1985).

²M. Vidic, S. M. Harb, and S. T. Smith, *Precis. Eng.* **22**, 19 (1998).

³C. P. Hendriks and W. P. Vellinga, *Rev. Sci. Instrum.* **71**, 2391 (2000).

⁴B. W. Chui, T. W. Kenny, H. J. Mamin, B. D. Terris, and D. Rugar, *Appl. Phys. Lett.* **72**, 1388 (1988).

⁵S. Phan, Ph.D. dissertation, University of North Carolina at Charlotte, 2000.

⁶R. G. Keanini, S. Phan, S. T. Smith, and R. J. Hocken, *Int. Comm. Heat Mass Transfer* **27**, 273 (2000).

⁷Y. Mitsuya, Y. Ohshima, and T. Nonogaki, *Wear* **211**, 198 (1997).

⁸S. T. Smith and D. G. Chetwynd, *Foundations of Ultraprecision Mechanism Design* (Gordon and Breach, London, 1992).

⁹R. J. Harker, *Generalized Methods of Vibration Analysis* (Wiley, New York, 1983).